Chemico-Biological Interactions 307 (2019) 167–178

Contents lists available at ScienceDirect

Chemico-Biological Interactions

journal homepage: www.elsevier.com/locate/chembioint

Polyethers isolated from the marine actinobacterium *Streptomyces cacaoi* inhibit autophagy and induce apoptosis in cancer cells

Nasar Khan[a,1], Sinem Yılmaz[b,c,1], Semiha Aksoy[d,1], Ataç Uzel[d], Çiğdem Tosun[a], Petek Ballar Kirmizibayrak[c,**], Erdal Bedir[e,*]

[a] Department of Molecular Biology and Genetics, Izmir Institute of Technology, Urla, 35430, Izmir, Turkey
[b] Department of Bioengineering, Faculty of Engineering, University of Alanya Aladdin Keykubat, Antalya, 07400, Turkey
[c] Department of Biochemistry, Faculty of Pharmacy, Ege University, Bornova, 35100, Izmir, Turkey
[d] Department of Biology, Faculty of Science, Ege University, Bornova, 35100, Izmir, Turkey
[e] Department of Bioengineering, Izmir Institute of Technology, Urla, 35430, Izmir, Turkey

ARTICLE INFO

Keywords:
Marine actinobacterium polyether antibiotic
Autophagy
Apoptosis

ABSTRACT

Polyether compounds, a large group of biologically active metabolites produced by *Streptomyces* species have been reported to show a variety of bioactivity such as antibacterial, antifungal, antiparasitic, antiviral, and tumour cell cytotoxicity. Since some of these compounds target cancer stem cells and multi-drug resistant cancer cells, this family of compounds have become of high interest. In this study, three polyether-type metabolites (**1**–**3**), one of which was a new natural product (**3**), were isolated from the marine derived *Streptomyces cacaoi* via antimicrobial activity-guided fractionation studies. As several polyether compounds with structural similarity such as monensin have been linked with autophagy and cell death, we first assessed the cytotoxicity of these three compounds. Compounds **2** and **3**, but not **1**, were found to be cytotoxic in several cell lines with a higher potency towards cancer cells. Furthermore, **2** and **3** caused accumulation of both autophagy flux markers LC3-II and p62 along with cleavage of caspase-3, caspase-9 and poly (ADP-ribose) polymerase 1 (PARP-1). Interestingly, prolonged treatment of the compounds caused a dramatic downregulation of the proteins related to autophagasome formation in a dose dependent manner. Our findings provide insights on the molecular mechanisms of the polyether-type polyketides, and signify their potency as chemotherapeutic agents through inhibiting autophagy and inducing apoptosis.

1. Introduction

Polyether compounds are potent antimicrobial and anticancer agents that belong to a large class of naturally occurring polyketides. A number of studies have revealed that the primary role of polyether ionophores such as monensin (Mon) and nigericin (Nig) is the loss of proton gradient across the membrane resulting in an increase of pH in lysosomes and blockage of lysosomal degradation [1]. It is well known that proper functioning of the lysosome is crucial for a healthy cellular life as it is involved in a variety of cellular pathways, especially autophagy, a conserved intracellular self-eating process and collection of extensive regulatory catabolic processes. Thus, autophagy is directly involved in cellular homeostasis and stress responses [2]. During autophagy, target proteins and organelles are sequestered in double membrane vesicles called the autophagosomes, which fuse with lysosomes to degrade its contents. Since autophagy plays a major role in cellular and organismal homeostasis, it is not surprising that aberrant autophagy has been associated with several pathologies including aging [3], cancer [4], neurodegeneration [5,6], myopathies [7], metabolic disorders [8], infections, immunity and inflammatory diseases [9,10].

Polyether ionophores have recently gathered attention in autophagy inhibition. It was reported that Mon and Nig treatment caused accumulation of autophagic vacuoles inside the cell [11] by inhibiting the terminal fusion stage of autophagy pathway along with the accumulation of autophagy flux markers LC3-II and p62 [12,13]. In addition, two polyether antibiotics, *viz.* salinomycin and maduramicin, were reported

Abbreviations: Mon, monensin; Nig, Nigericin; Baf A1, Bafilomycin A1; Doxo, Doxorubicin; MDC, Monodansylcadaverine; DMSO, Dimethyl sulfoxide; EtOH, Ethanol; NMR, Nuclear magnetic resonance; TLC, Thin-layer chromatography

* Corresponding author.
** Corresponding author.
E-mail addresses: petek.ballar@ege.edu.tr (P.B. Kirmizibayrak), erdalbedir@iyte.edu.tr (E. Bedir).
[1] These authors equally contributed to this manuscript.

https://doi.org/10.1016/j.cbi.2019.04.035
Received 6 February 2019; Received in revised form 20 April 2019; Accepted 30 April 2019
Available online 03 May 2019
0009-2797/

to inhibit the autophagic flux in several cancer cell lines [14,15]. Since several autophagy inhibitors raise lysosomal pH and disrupt autophagy flux, they have been used as autophagy inhibitors in cultured cells [16,17]. However, only chloroquine and its derivative hydroxychloroquine (HCQ) have set the stage for clinical trials examining their therapeutic effects [18].

While three distinct cell death pathways have been elucidated (apoptosis, controlled necrosis and autophagic cell death), these pathways do not work in a mutually exclusive manner, but rather cells undergo mixed features of multiple cell death mechanisms. Several groups have recently engaged in the crosstalk between autophagy and apoptosis. The studies on polyether ionophores as potential anticancer molecules revealed that these agents might target both autophagy and apoptosis [13,15,19,20]. Thus, polyether antibiotics are emerging as novel potential anticancer compounds. Salinomycin for example induces massive apoptosis in several cancer cells, but not in normal cells, such as human T lymphocytes [21]. Furthermore, salinomycin pretreatment resulted in a 100-fold decrease of epithelial cancer stem cells when compared to paclitaxel treatment in breast cancer cell lines [22]. In addition to their robust effects of monotherapy in cancer, concurrent therapies of polyether antibiotics along with other anticancer agents have been utilized to increase treatment efficiency in resistant cancer cell lines [23,24]. Polyether antibiotics Mon, Nig, salinomycin, narasin and lasalocid have shown to restore the sensitivity of malignant glioma cells towards TRAIL mediated apoptosis by triggering ER stress, CHOP mediated DR5 upregulation and c-FLIP downregulation by proteasomal degradation [23]. Similarly, combination treatment of Mon with anticancer drugs like rapamycin (mTOR inhibitor) or erlotinib (epidermal growth factor receptor inhibitor) resulted in an improved synergistic anticancer activity in lung cancer cell line [19].

The Mediterranean Sea is one of the global biodiversity hotspots [25]. However, the rich biodiversity of the Mediterranean Sea, has not been studied intensely for the presence of marine actinobacteria and for their bioactive compounds [26]. A strain isolated from Mersin sediment samples (The East Mediterranean Coastline, Turkey) was identified as *Streptomyces cacaoi*. The ethyl acetate extract of the *S. cacaoi* fermentation broth exhibited an interesting chemical profile and noteworthy antimicrobial activity in our preliminary screenings. Large-scale fermentation studies followed by fractionation and purification studies resulted in the isolation of three metabolites (**1**–**3**). As the purified molecules turned out to be polyether-type metabolites after spectral characterization, we directed our efforts towards the cytotoxicity of these compounds and their activities on autophagic pathway. Our data showed that compounds **2** and **3** displayed cytotoxicity in several cell lines with a higher potency towards cancer cells. The effect of compounds **2** and **3** on the autophagy and apoptosis was evaluated by the levels of autophagy related proteins LC3-II, p62/SQSTM1 and ATG proteins under different conditions and by the cleavage of apoptotic markers such as PARP-1, caspase-3, caspase-8, and caspase-9, respectively. Our results postulate substantial data on the apoptotic and autophagic effects of the polyethers.

2. Experimental procedures

2.1. General experimental procedures

MS data was acquired on a Thermo Scientific Accela1250 system consisting a mass detector (Thermo Scientific TSQ Quantum Access Maxx triple quadrupole). The mass analysis samples were dissolved in dichlorometane:methanol (1:1) at 10 ppm concentration, and 10 μL of this solution was directly injected to the instrument (Capillary Temperature: 400; Vaporizer Temperature: 500.0; Sheath Gas Pressure: 75.0; Ion Sweep Gas Pressure: 0.0; Aux Valve Flow: 20.0; Spray Voltage: Positive polarity - 3000.0, Negative polarity - 3000.0; Discharge Current: Positive polarity - 4.0, Negative polarity - 4.0). 1D and 2D NMR spectra were obtained at 400 MHz for ^{1}H and 100 MHz for ^{13}C on a Varian Oxford AS400 spectrometer, in $CDCl_3$, with solvent peak used as reference. Column chromatography experiments were carried out on silica gel 60 (40–63 μm-Merck). TLC analyses were carried out on Silica gel 60 F254 (Merck) and RP-18 F254s (Merck) plates. Compounds were detected by UV and 20% aq. H_2SO_4 spraying reagent followed by heating at 105 °C for 1–2 min. For rotary evaporation, a Heidolph Laborota 4001 equipment was used.

2.2. Sampling location and isolation of marine actinobacterium isolate

A sediment sample obtained from Mersin Coastline (Turkey) at a depth of 8 m, was used for the isolation of actinobacteria using M6 medium [g/L: yeast extract, 1.0; meat extract, 4.0; peptone, 4.0; glucose, 10.0; NaCl, 20.0 and agar, 20.0, pH 7.5) according to the method of Maldonado et al. [27].

2.3. Characterization of the actinobacterium isolate

DNA isolation was carried out according to a slightly modified method of Liu et al. [28]. Sequencing of 16S rRNA region was used for identifying the isolate by using universal primers 27F and 1492R. The amplification reaction was carried out as described previously [29]. The sequence (JX912350.1) obtained from sequencing on an ABI 3130XL automated sequencer (Applied Biosystems) was pairwise matched and aligned with the sequences retrieved from GenBank, NCBI.

2.4. Preliminary fermentation

Liquid M6 medium was used for production of antimicrobial substances and fermentation was performed at 28 °C and 150 rpm for 14 days. Every 4 days from 2 to 14, 25 mL of fermentation broth was taken and ethyl acetate extraction was performed. Activities of the extracts were determined on Mueller Hinton Agar (MHA) by using disc diffusion method against four bacteria (*E. faecium* DSM13590: vancomycin-resistant; *Escherichia coli* O157:H7 RSKK234: streptomycin-, sulfisoxazole-, and tetracycline-resistant; *S. aureus* DSM11729: methicillin-resistant; *Pseudomonas aureginosa* ATCC27853) and a yeast species (*C. albicans* DSM5817).

2.5. Large-scale fermentation

An inoculum of culture of *S. cacaoi* 14CM034 was aseptically added to an Erlenmeyer flask (250 mL) containing 50 mL M6 medium. The culture was incubated at 28 °C using a shaker at 150 rpm. After 72 h of incubation, 5 mL of culture medium was transferred to Erlenmeyer flasks (1 L) containing 200 mL liquid M6 medium and the flasks was incubated at 28 °C and 150 rpm. Incubation was stopped after 10 days, and, in total, 50 L of fermentation liquid was obtained after removal of cells by centrifugation. The fermentation broth was extracted with ethyl acetate three times to yield 4.53 g extract (0.091 g/L yield) after evaporation at 40 °C in vacuo.

2.6. Bioassay-guided fractionation

Analytical TLC was performed on silica gel plates (Silica gel 60 F254, 0.2 mm, Merck, Darmstadt, Germany) to compare chemical contents of fractions showing antimicrobial behavior and to establish solvent systems for chromatographical separations. The solvent systems used were $CHCl_3$:MeOH (9:1), $CHCl_3$:MeOH:H_2O (85:15:0.5, 80:20:2, 70:30:3, 61:32:7), Ethyl acetate:MeOH:H_2O (100:17.5:13.5) and Hexane:Ethyl acetate:MeOH (10:10:2 and 10:10:3). For detailed isolation procedures *see* Fig. S1 in the supplementary file.

2.7. Isolation of Mon (positive control)

A commercial animal feeding product having local name

"Elancoban 200" was purchased from the veterinary medicine shop, containing 23.6% Mon sodium salt. The granule product (20 g) was extracted with Water: Ethyl acetate (1:1) in a separation funnel. The upper organic layer was concentrated by rotatory evaporation giving a semisolid pasty residue. This extract was subjected for purification to open column chromatography (Silica gel 60, 120 g) employing $CHCl_3$:MeOH:Acetone:Glycerol (98:20:40:2) as mobile phase. Fractions from 77 to 92 were pooled together, and after evaporation, it was purified by open column chromatography (Silica gel 60, 80 g) using ethyl acetate as mobile phase to afford Mon. Purity and authenticity of the isolate was confirmed by ^{1}H NMR experiment [30].

2.8. Broth microdilution method

Minimum inhibitory concentrations (MIC) of the purified compounds (Table S1) were performed by the microdilution method described earlier [31].

2.9. Cell culture and drug treatment

Human endometrial carcinoma (HeLa), human prostate adenocarcinoma (PC-3), human lung adenocarcinoma (A549), human colorectal adenocarcinoma (CaCo-2), human lung fibroblasts (MRC-5) and *Cercopithecus aethiops* kidney cell lines (Vero) were obtained from American Type Culture Collection and maintained as exponentially growing monolayers by culturing according to the supplier's instructions. For cytotoxicity analysis, each cell line was exposed to compounds (**1–3**) at a final concentration of 2.5, 5, 10, 25 and 50 μM for 48 h. For immunoblotting experiments, cells were treated with the IC_{50} values of compounds for 6 and/or 24 h to evaluate early and late response. In dose response studies, cells were incubated 24 h with ¼, ½, 1 and 2X of IC_{50} value of **2** and **3**. In Bafilomycin A1 (Baf A1) combination experiment, HeLa cells were co-treated with 100 ng/ml Baf A1 (CST, US) and IC_{50} values of **2** and **3** for 4 h. For Monodansylcadaverine (MDC) fluorometry analysis HeLa cells were treated with IC_{50} value of **2**, **3** and Mon for 24 h.

2.10. Cytotoxicity analysis

After cells were incubated for 48 h with compounds, the mixture of WST-1 (Roche, Switzerland) and medium (1:9) was replaced with old media in each well. Absorbance was measured with a microplate reader at 440 nm (Varioscan, Thermo Fisher Scientific, US) after incubating cells for 0.5-, 1-, 2-, 3 and 4 h at 37 °C respectively. Doxorubicin (Doxo) (CST; US) was used as a positive control for this assay, while the solvents were used as negative controls; ethanol (EtOH) for **3** or Mon, and dimethyl sulfoxide (DMSO) for **1** or **2**. Cytotoxicity data were fitted to a sigmoidal curve, and a four-parameter logistic model in Graph Pad Prism 5 (San Diego, CA, US.) was used to calculate the IC_{50}, which represents the concentration of compound that is required for 50% inhibition in comparison to solvent-treated controls. The IC_{50} values were reported with ± 95% confidence intervals (± 95% CI).

2.11. Western blot analysis

Cells were harvested and lysed with RIPA buffer (50 mM Tris-HCl, pH 8.0, 1% NP-40, 0.1% SDS, 150 mM NaCl, 0.1% Triton X-100, 5 mM EDTA) with protease inhibitors (Roche, Switzerland) to prepare whole cell lysates following treatments. Protein concentrations were determined by bicinchoninic acid (BCA) protein assay (Thermo Fisher Scientific, US). Equal amounts of proteins were loaded to the gels and proteins were separated by SDS-PAGE electrophoresis and transferred to PVDF membranes (EMD Milipore, Thermo Fisher Scientific, US). Membranes were blocked in PBS–0.1% Tween-20 with 5% non-fat dry milk. Mouse monoclonal antibodies used in this study were anti-caspase-9 (CST-9508, US), anti-caspase-8 (CST-9746, US), anti-GFP (SC-9996), and anti-actin (Sigma-Aldrich-A5316, UK). The rabbit monoclonal antibodies used in this study included anti-LC3 (CST-12741, US), anti-Atg3 (CST-3415, US), anti-Atg5/12 (CST-12994, US), anti-Atg7 (CST-8558, US), anti-Atg16L1 (CST-8089, US), anti-caspase-3 (CST-9665, US), anti-PARP-1 (CST-9542, US). Anti-p62 (Proteintech-184201AP, USA) and anti-Beclin 1 (Proteintech-113061AP, USA) were rabbit polyclonal antibodies. Species-specific horseradish peroxidase (HRP)-coupled secondary antibodies were used (goat anti-rabbit and goat anti-mouse, Thermo Fisher Scientific, US). Chemiluminescence signals were detected using Clarity ECL substrate solution (BIORAD, US) by Fusion-FX7 (Vilber Lourmat, Thermo Fisher Scientific, US).

2.12. Transfection and fluoresence microscopy

HeLa cells on a 100 mm dish were transfected with GFP-LC3 expression construct using Lipofactamine 3000 (Thermor Fisher, USA) according to the manufacturer's protocol. Next day cells were split on 12 wells with or without coverslips for fluorescence microscopy or immunoblotting, respectively. At the end of treatments cells on coverslips were washed twice with ice cold PBS and fixed with 4% paraformaldehyde in PBS for 30 min at 4 °C. After washing 5 times with PBS, mounted samples were analyzed by fluorescence microscopy (Olympus IX70, Japan). For quantification of autophagic cells, GFP-LC3 punctuated dots were determined from triplicates by counting a total of more than 30 cells [32].

2.13. MDC fluorometric analysis

After HeLa cells were treated with compounds, they were washed 2 times with 1X PBS followed by a 10 min incubation with 50 μM MDC in 1X PBS at 37 °C. After 3 washes in PBS, MDC fluorescence intensity was immediately measured with a microplate reader (Varioscan, Thermo Fisher Scientific, US) using excitation/emission maxima 365nm/525 nm. Cells were then first treated with 0.02% TritonX-100 in PBS for 10 min and then incubated with 100 μg/ml Propidium Iodide (PI) for 15 min at room temperature. Finally, the plate was read again by multiplate reader (Varioscan, Thermo Fisher Scientific, US) using excitation/emission maxima 535nm/617 nm. After blank subtraction, MDC values were normalized with PI values and the relative MDC specific activity was determined for each sample compared to negative controls (EtOH and DMSO). Fluorometric analysis of MDC was performed in triplicates and quantitative data was presented as mean ± standard error of mean (s.e.m). Data was analyzed by one-way analysis of variance (ANOVA) followed by Turkey's post-hoc test. Statistical analysis was performed using Origin Pro (V8, OriginLab) software.

3. Results

3.1. Isolation and structure elucidation of compounds 1-3

The isolation studies were performed using a Mediterranean sediment sample, which provided a bioactive actinobacterium 14CM034. The isolate exhibited significant antimicrobial activity against methicillin resistant *S. aureus* (18 mm), *E. faecium* (23 mm) and *C. albicans* (14 mm) in the disc diffusion assays. Sequencing using primers 27F and 1492R revealed that the isolate was a member of *Streptomyces* genus. When the molecular identification evaluated with the phenotypical results, the isolate was identified as *S. cacaoi*. Large-scale fermentation of *S. cacaoi* provided 4.53 g of ethyl acetate extract. Bioassay-guided fractionation of the ethyl acetate extract led to the isolation of three compounds (**1–3**), of which **1** (arenaric acid) and **2** (K41 A) were identified as polyether-type polyketides, by comparison of their spectral data with those previously reported (Fig. 1A) [33–36].

The TLC spot observed for compound **3** was monitored under UV light and after spraying aq. sulfuric acid, which implied its polyether character as in **1** and **2**. Structure of **3** was determined using spectral

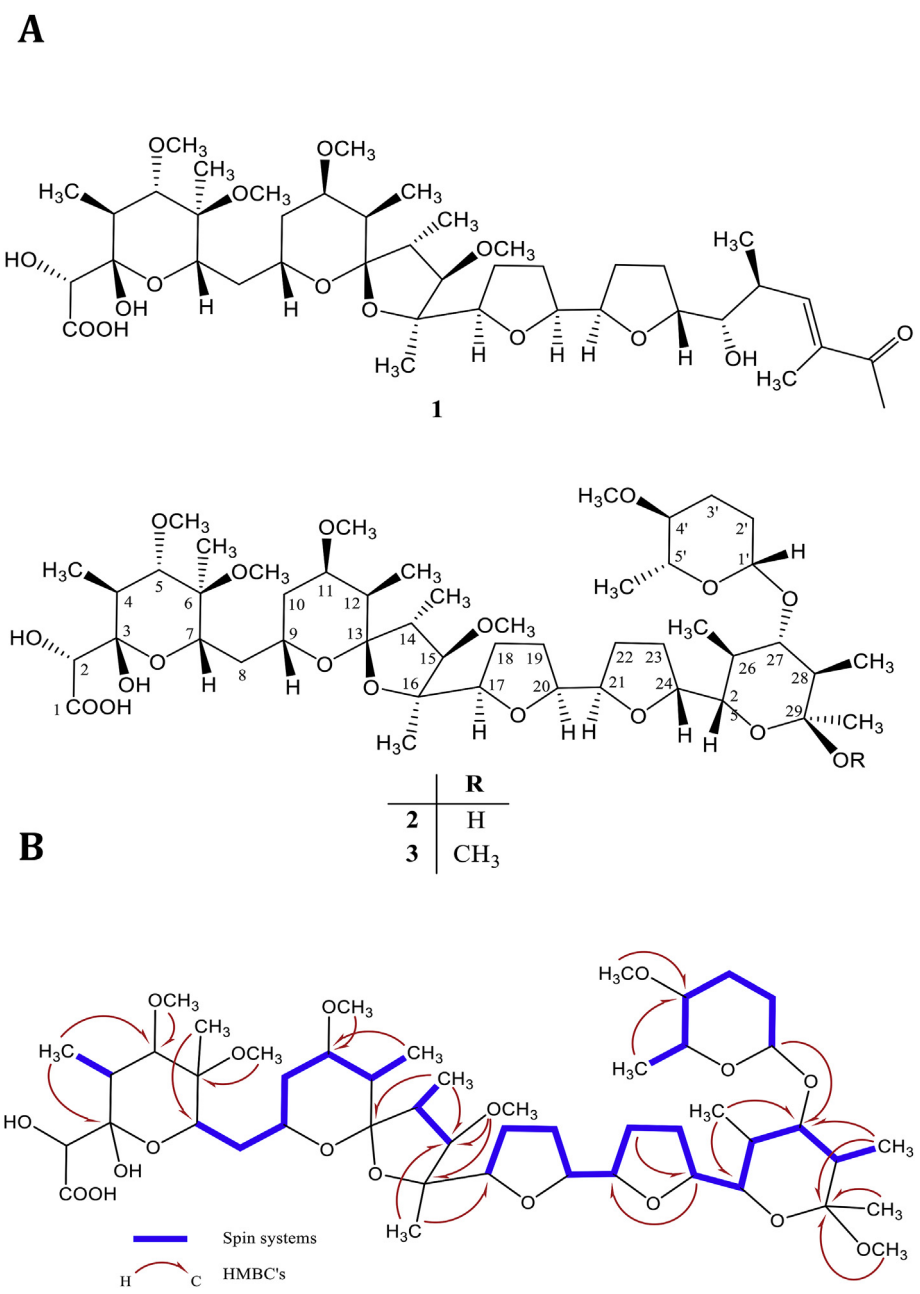

Fig. 1. A. Structures of three polyether compounds (**1–3**) isolated from the marine actinobacterium *Streptomyces cacaoi*. **B.** Spin systems deduced from COSY spectrum and key HMBC's for compound **3**.

methods (MS, 1D and 2D-NMR). The ESI-MS analysis of **3** (*m/z* 960.0 $[M]^-$, negative mode; 978.4 $[M + NH_4]^+$, positive mode) suggested a 14 amu increase compared to compound **2** (*m/z* 946.0 $[M]^-$, negative mode; 964.4 $[M + NH_4]^+$, positive mode). In the ^1H and ^{13}C NMR spectra of **3**, the resonances were almost superimposable with those of compound **2** (Table 1), except additional signals originating from an *O*-methyl group [δ_H 3.12, s; δ_C 48.7], which was also explaining the mass difference between **3** and **2** (Fig. 1A). Inspection of the COSY and HMQC spectra revealed five spin systems as in **2**: i) H-4 to Me-4; ii) H-7 to Me-12; iii) Me-14 to H-15; iv) H-7 to Me-28; v) H-1′ to Me-5′ (Fig. 1B). Based on the HMBC correlations of **3**, positions of the spin systems, quaternary carbons and methyl groups were established, and the same framework with that of **2** was confirmed. The position of the additional methyl group was determined to be C-29(O) on the basis of the long-range correlation from δ_H 3.12 to C-29 (δ_C 101.0) (Fig. 1B). Thus, the structure of **3** was elucidated as 29-*O*-methyl derivative of K41 A (**2**). Compound **3** was synthesized early in 1970's starting from K41 A (**2**) by a pharmaceutical company and registered under the patents US4303647 and US4331658 for its potent anti-coccidiosis and anti-dysenteric activity. Thus, herein, **3** is being reported for the first time as a new natural product.

3.2. Compounds 2 and 3 have higher potency against cancer cells

In this study, we first evaluated the cytotoxic activity of these three compounds by using WST-1 assay in human cancer cell lines, *viz.* CaCo-2, HeLa, PC-3, and A549, and compared them to normal cell lines, MRC-5 and Vero (Table 2). Our results revealed that compound **1** did not show any significant cytotoxicity, whereas **2** and **3** inhibited cell proliferation with a higher selectivity on cancer cells when compared to non-cancer cell lines. In this experiment, we used Mon, the well-characterized polyether antibiotic, and doxorubicin as positive controls.

Table 1
^{1}H and ^{13}C NMR Data of Compound **3** (in $CDCl_3$ at 400 MHz; δ in ppm, J in Hz) and ^{13}C NMR Data of **2** from Ref. [36].

Position	3		2
	δ_C	δ_H (J in Hz)	δ_C
1	178.7	–	178.4
2	71.4	3.87 s	71.8
3	99.3	–	98.2
4	38.8	2.17 m	38.7
5	85.7	3.36 m	85.5
6	78.6	–	78.5
7	66.7	3.85 m	66.7
8	32.5	1.55 m	32.5
9	62.0	3.92 m	61.3
10	31.3	1.16 m, 2.15 m	31.27
11	79.6	3.35 m	79.7
12	37.2	1.79 m	36.9
13	107.3	–	106.8
14	46.8	2.16 m	46.2
15	95.2	3.52 d (9.1)	94.5
16	84.4	–	83.3
17	83.4	3.82 m	83.6
18	26.2	1.82 m, 1.92 m	23.2
19	23.4	1.51, 1.72 m	no assignment
20	81.5	3.75 ddd (10.1, 5.1, 2.3)	79.3
21	78.8	4.84 dt (8.4, 3.1)	79.3
22	28.6	1.49 m, 2.29 m	29.2
23	24.6	1.78 m, 2.04 m	24.3
24	81.6	4.45 d (8.3)	80.3
25	78.2	3.60 d (10.8)	74.3
26	38.9	2.18 m	39.1
27	82.9	3.37 m	82.8
28	47.9	1.51 m	47.0
29	101.0	–	98.2
1'	102.9	4.41 dd (9.4, 1.8)	102.5
2'	30.7	1.47 m, 1.95 m	30.6
3'	27.5	1.31 m, 2.14 m	25.7
4'	80.0	–	80.7
5'	74.27	3.28 m	74.3
4-Me	12.3	1.08 d (6.6)	12.3
5-OMe	61.2	3.56 s	60.9
6-Me	11.3	1.16 s	11.1
6-OMe	50.9	3.37 s	50.8
11-OMe	59.1	3.42 s	59.2
12-Me	12.6	0.99 d (6.4)	12.7
14-Me	11.9	1.03 d (6.8)	11.7
15-OMe	60.3	3.41 s	60.2
16-Me	28.5	1.61 s	28.5
26-Me	13.7	1.02 d (6.4)	13.6
28-Me	12.9	0.98 d (6.4)	12.7
29-Me	22.2	1.24 s	27.0
29-OMe	48.7	3.12 s	–
4′-OMe	57.0	3.35 s	56.7
5′-Me	18.5	1.23 d (5.5)	18.4

Similar to compounds **2** and **3**, both Mon and doxorubicin preferentially targeted cancer cells (Table 2). Furthermore, **2** had potency against colorectal and prostate cancer cell lines with the IC_{50} values of 7.43 and 11.76 μM, respectively, whereas **3** displayed modest toxicity on PC-3 and CaCo-2 cells (IC_{50} = 23.76 and 27.89 μM, respectively). Taken together, it was found that cancer cells were more susceptible especially to Mon and **2**; however, the activity varied among cell lines.

3.3. Compounds 2 and 3 block autophagic flux

Several reports have linked polyethers to autophagy [16,17]. Therefore, we wanted to investigate the effect of compounds **2** and **3** on autophagy. During autophagy, LC3-I is processed and recruited to phagophores, whereas LC3-II is generated by site-specific proteolysis and lipidation [37]. Although the characteristic conversion from endogenous LC3-I to LC3-II is commonly used to monitor autophagosome formation, it is not sufficient for the proper evaluation of autophagic flux since both autophagy activation and inhibition of autophagosome degradation greatly increases the amount of LC3-II [38,39]. The levels of p62/SQSTM1 protein, which is involved in promoting the turnover of protein aggregates following polyubiquitination, is another commonly used marker to detect autophagy activity due to its interaction with LC3 and selective degradation by autophagy [40]. If the autophagic flux or autophagic degradation activity is blocked, both LC3-II and p62/SQSTM1 are accumulated [38]. Thus, we examined the protein expression levels of LC3-II and p62/SQSTM1 on CaCo-2, PC-3 and HeLa cells treated with compounds **2** and **3** at concentrations equivalent to their IC_{50} values either for either 6 or 24 h (Fig. 2A and B). We used Baf A1 as an autophagy inhibitor since it inhibits lysosomal degradation by decreasing the acidification of lysosomes via inhibiting vacuolar type H^+ ATPase (V-ATPase) and blocking the fusion of autophagosomes with lysosomes. Mon, a previously reported polyether antibiotic was also included as an inhibitor of autophagy at the fusion step. We observed that 6 h treatment of compounds **2** and **3** is sufficient to increase LC3-II and p62 (Fig. 2A). We further detected a pronounced increase in the LC3-II and p62 levels when cells were incubated both with **2** and **3** for 24 h (Fig. 2B). Together, our findings suggest that both compounds **2** and **3** have an effect on the autophagy process initially at 6 h and have more profound effects at 24 h.

The difference in the amount of LC3-II protein levels between compound treated samples with and without lysosome inhibitor represents the level of autophagic flux [39]. Thus, we next investigated the integrity of the autophagic flux upon treatment of compounds **2** and **3** in the presence or absence of Baf A1. While **2** or **3** increased LC3-II levels in the absence of Baf A1, this increase was not exacerbated in the presence of Baf A1, indicating that these compounds impaired autophagic flux (Fig. 3A). We also utilized GFP-LC3 puncta formation assay which enabled us to determine the average number of punctate structures per cell by fluorescence microscopy. The difference in the number of LC3 puncta of the compound treated cells with and without lysosome inhibitor reflects autophagosome degradation during the treatment period [39]. We incubated cells with compound **2** and Mon and found that the number of LC3 puncta was increased when compared to the control cells. However, the combination of compounds with Baf A1 did not further enhance the number of puncta (Fig. 3B). Thus, our data suggest that tested compounds likely block LC3-II degradation, which could be due to the aberrant transport to the lysosome or degradation in the lysosome rather than the promotion of autophagic vacuoles formation. We also measured the turnover rate of GFP-LC3 by determining

Table 2
IC_{50} values (μM) of the polyether antibiotics against cancer and non-cancerous cell lines. ND: Not determined at tested concentrations.

Compound	Cancer Cell line				Non-cancerous Cell line	
	HeLa	CaCo-2	PC-3	A549	MRC-5	Vero
1	ND	ND	ND	ND	ND	ND
2	23.7 ± 0.3	7.4 ± 0.3	11.8 ± 0.6	23.2 ± 1.3	35.2 ± 0.9	23.3 ± 0.6
3	32.6 ± 0.1	27.9 ± 0.5	23.9 ± 1.8	26.9 ± 0.9	39.9 ± 0.8	39.7 ± 0.4
Mon	11.9 ± 0.2	9.4 ± 1.1	8.4 ± 1.5	20.1 ± 0.3	45.9 ± 1.4	> 50
Doxo	1.2 ± 0.2	8.8 ± 0.3	1.7 ± 0.3	1.1 ± 0.1	> 5	> 5

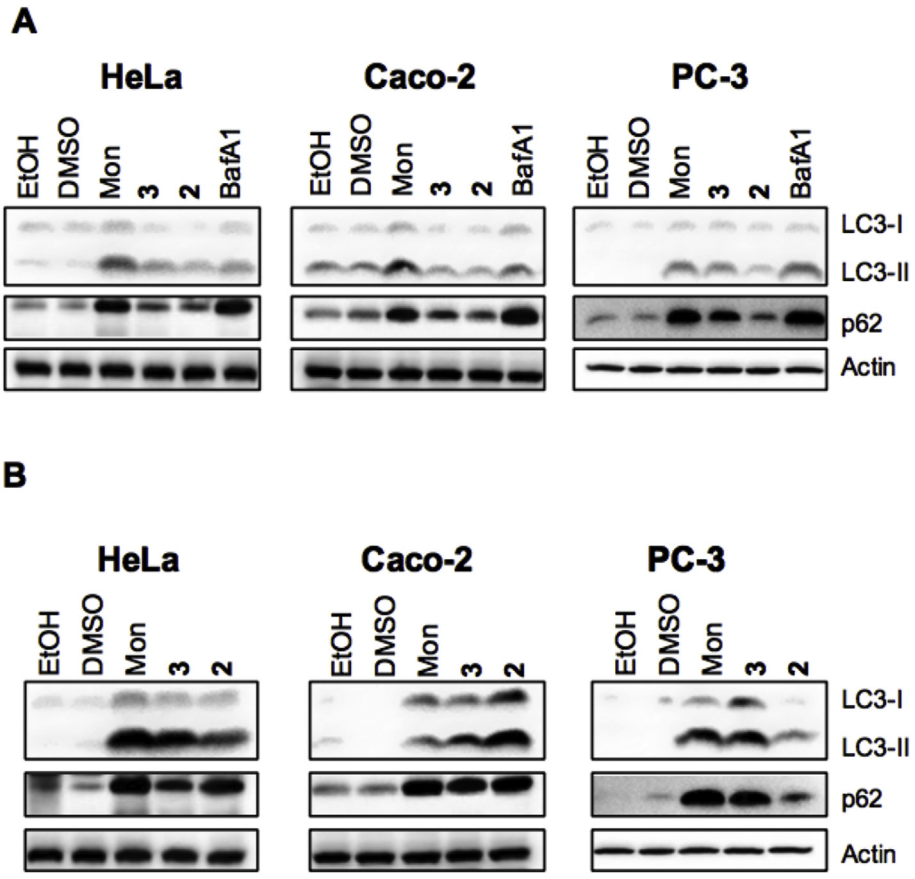

Fig. 2. Compounds **2** and **3** inhibit autophagy in several cell lines. HeLa, Caco-2 and PC-3 cells were treated with compounds **2**, **3** and Mon at IC_{50} concentrations either for **(A)** 6 h and **(B)** 24 h Conversion of LC3-I to LC3-II was detected by immunoblotting (IB) with the antibody against LC3. p62 levels were evaluated with anti-SQSTM1/p62 antibody. Actin was used as housekeeping control. Baf A1 was used at 100 ng/ml. The experiments were repeated three times independently; with one representative result shown.

the free GFP fragments. Interestingly, while neither starvation nor Baf A1 caused accumulation of the free GFP levels when compared to the control samples, compound **2**, at IC_{50} and 2 fold IC_{50} values, and Mon enhanced free GFP levels (Fig. 3C). Our findings on the effect of starvation and Baf A1 on the GFP-LC3 turnover are in parallel with a previous report suggesting that cleavage of free GFP from GFP-LC3 can occur depending on the autophagic stimuli, the extent of lysosomal inhibition and the change in lysosomal pH [32]. Interestingly, we obtained contradictory results on two tested autophagy inhibitors, where Mon but not Baf A1 caused the accumulation of free GFP. A similar paradox was previously reported for chloroquine and Baf A1 [32]. It was shown that chloroquine at unsaturating concentrations increased free GFP levels, but at higher saturating concentrations did not cause the accumulation of free GFP. These data suggest that GFP-LC3 fusion protein is degraded in a step-wise fashion, where the LC3 portion is degraded at a faster rate than GFP. Therefore, we suggest that the concentration used for **2**, **3** and Mon are unsaturated doses and not sufficient to completely suppress the lysosomal function unlike 100 nM of Baf A1. We were not able to test the saturated concentrations, which were above 2 x IC_{50} values, due to solubility limitations of our compounds.

In order to evaluate the effect of **2** and **3** on the levels of key autophagy proteins, we treated HeLa and CaCo-2 cell lines with the compounds (Mon, **2** and **3**) for 6 and 24 h at concentrations equivalent to their IC_{50} values, and examined the level of proteins of interest by immunoblotting (IB). While 6 h treatment of **2** and **3** had either no or only a moderate decrease on Atg5-12, Atg7 and Beclin-1 proteins in HeLa cells, the expression level of these proteins drastically diminished at 24 h treatment (Fig. 4A). We observed a similar pattern in Caco-2 cells, where Atg5-12, Atg7 and Beclin-1 levels were decreased at 24 h but not at 6 h (Fig. 4B). Surprisingly, Mon did not show any significant effect on Beclin-1 and the Atg proteins over the times tested (Fig. 4A and B). Moreover, we detected a dose-dependent downregulation of Atg proteins following 24 h treatment of **2** and **3** (Fig. 4C). Our results suggest that prolonged treatment of **2** and **3**, but not Mon decreased levels of Atg proteins that is required for autophagic vesicle maturation.

Even though Mon, **2**, and **3** have polyether-type backbones, we identified some differences in their mechanisms where **2** and **3** but not Mon diminishes the level of autophagy proteins after prolonged exposure. In a different experimental setup, we investigated the effect of these compounds on acidic compartments in HeLa cells by fluorometry analysis of MDC, a fluorescent dye specific for the acidic compartments (Fig. 5). Both Mon and Baf A1 demolished the fluorescence intensity of MDC staining, which is consistent with the previous reports where Baf A1 demolished the acidic pH in intercellular compartments [41,42]. On the other hand, we detected a significantly enhanced MDC fluorescent intensities in cells treated with **2** and **3,** suggesting the accumulation of acidic autolysosomes rather than neutral autophagosomes.

3.4. Polyether antibiotics induce apoptosis

Recently, the interrelationship between autophagy and apoptosis has been undertaken by many groups [43,44]. While autophagy and apoptosis can act in a cooperative manner to invoke cell death in some cases, they can also work in a disparate manner to antagonize each other [45,46]. Therefore, we also tested the effect of compounds **2** and **3** on apoptosis. Compounds **2** and **3** triggered a dose dependent cleavage of PARP-1, a hallmark of caspase-dependent apoptosis (Fig. 6A and B). Since PARP-1 cleavage is considered to be a consequence of caspase activation, we further investigated the effect of compounds **2** and **3** on the intrinsic and extrinsic apoptotic pathways by detecting full length and cleaved fragments of predominant apoptosis executor caspases, namely Caspase −3, −8 and, −9 (Fig. 6C). Treatment of compounds **2** and **3** for 24 h with their IC_{50} concentrations increased the cleaved caspase-9 and -3 fragments (Fig. 6C). On the other hand, we did not detect cleaved caspase-8 in cells treated with compound **2**,

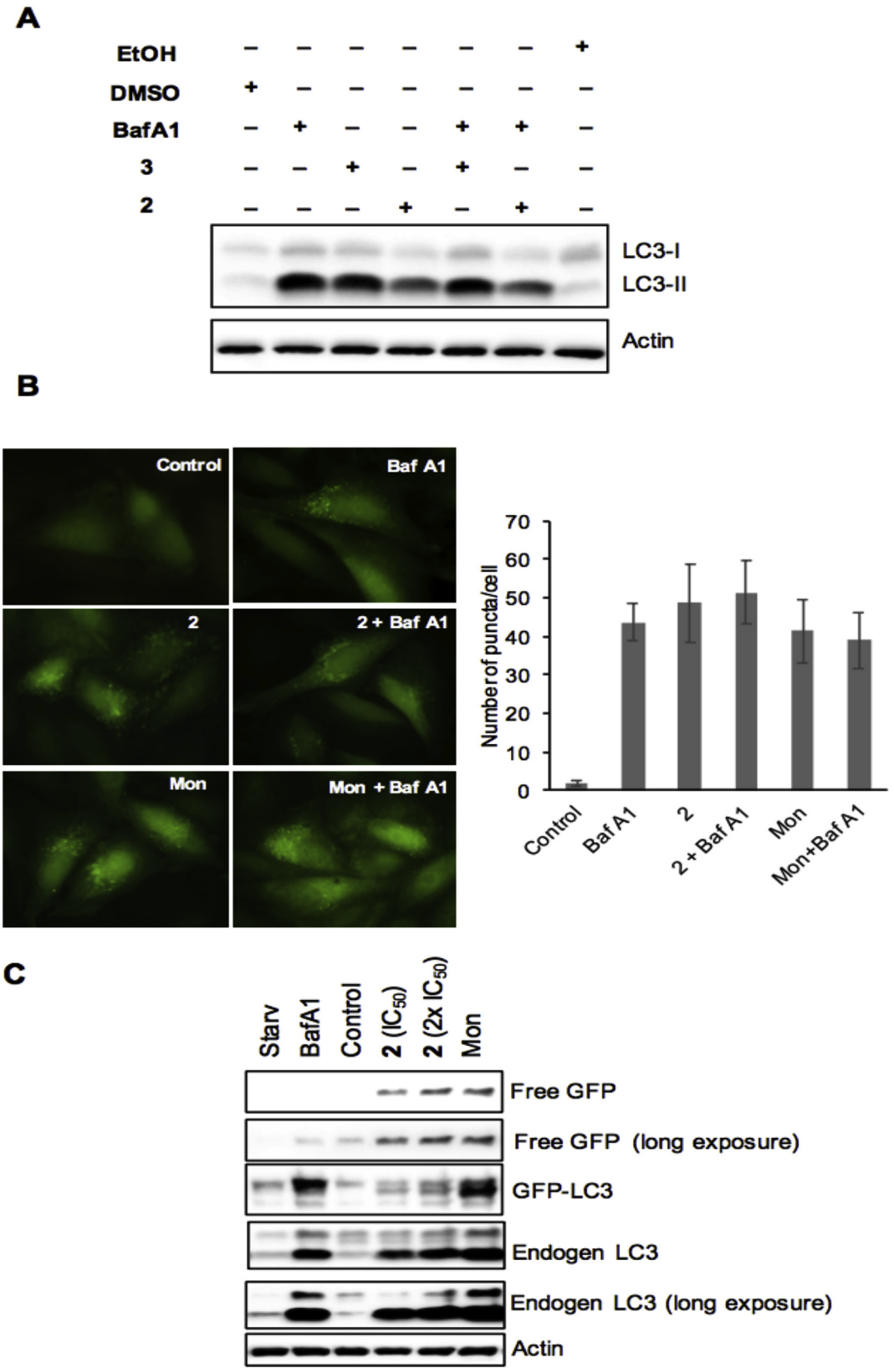

Fig. 3. Compounds **2** and **3** impair the integrity of autophagy flux. **A.** HeLa cells were treated with the compounds **2** and **3** alone at IC_{50} concentrations for 24 h or in combination with Baf A1 (100 nM) at the last 4 h. The levels of LC3-I, LC3-II and actin were detected by IB. Representative data from three independent experiments are shown. **B.** HeLa cells transfected with GFP-LC3 plasmid were treated with the compounds **2** and Mon alone at IC_{50} concentrations or in combination with Baf A1 (100 nM) for 4 h. Starvation and Baf A1 alone treatments were used as positive controls. The GFP-LC3 puncta structures were visualized by flouresence microscopy and representative data are shown. The quantification was done as described in Methods section. **C.** In GFP-LC3 turnover assay, GFP-LC3 transfected HeLa cells were treated with compounds at indicated concentrations for 24 h and then total lysed lysates were prepared and subjected to immunoblotting analysis. Representative data from four independent experiments are shown.

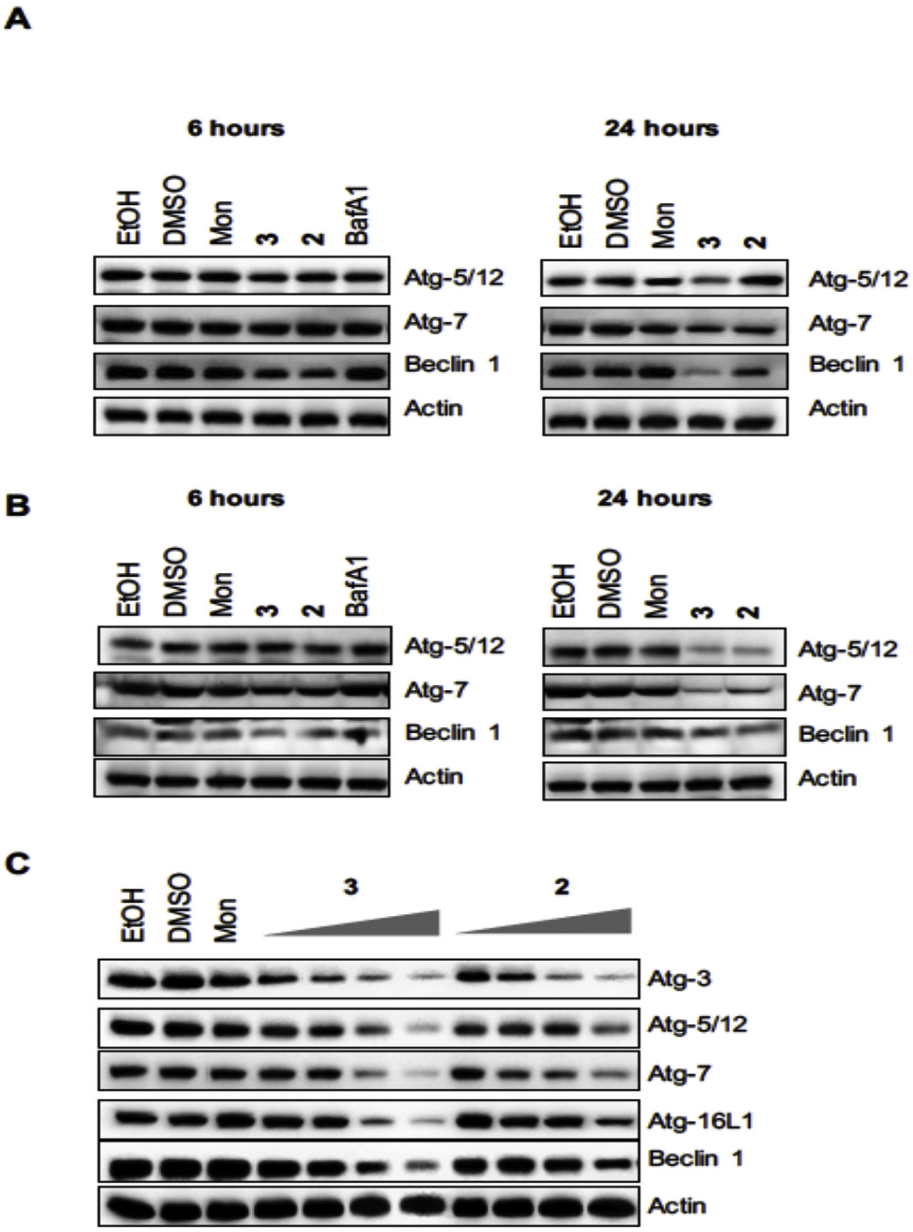

Fig. 4. Prolonged treatments of **2** and **3**, but not Mon downregulate ATG genes in a dose dependent manner. **(A)** HeLa and **(B)** CaCo-2 cells were incubated with compounds **2**, **3** and Mon at IC_{50} concentrations for 6 h or 24 h. The levels of Atg-5/12, Atg7 and Beclin1 were detected by IB using antibodies against them. Actin was used as loading control. **C.** ¼, ½, 1X and 2X of IC_{50} doses of compounds **2** and **3** were used in dose-dependency experiment. The expression of autophagy related ATG genes was evaluated by IB. The experiments were repeated three times independently; with one representative result shown.

suggesting that of our purified isolates can specifically induce the intrinsic apoptosis pathway.

4. Discussion

There is an increased interest in polyether ionophores and to date more than 120 naturally occurring ionophores have been characterized [47]. Major use of these compounds is against coccidiosis by targeting the ruminal bacterial population and today seven carboxylic ionophores are marketed in the USA for poultry and growth promotion in ruminants [48].

Arenaric acid (**1**), a rare polyether compound obtained from marine actinobacteria, was the first polyether compound isolated in this study [49]. The other known compound, K41 A (**2**), is one of the first isolated polyether antibiotics, and its bioactivities has been extensively evaluated [50,51]. The antimalarial effects of K41 A against resistant *Plasmodium* species (K1 and FCR3 strains) were found to be as competitive as artemether and artesunate (IC_{50} = 8.5–31 nM), currently used semi-synthetic natural products in the treatment of malaria [52]. In our antimicrobial activity tests, K41 A (**2**) was the most effective compound with MIC values of 0.11, 1.79 μg/mL against MRSA and *E. faecium*, respectively, while compound **3** had the highest activity against *C. albicans* at 4.0 μg/mL dose (Table S1). Additionally, all the compounds were found to be moderately active against *E. coli* (*ca.* 16 μg/mL). It is well known that the ionophore polyethers are most effective against Gram-positive bacteria. Cell membrane of this group of bacteria is surrounded by the peptidoglycan layer that is porous, and allows small molecules to pass through, reaching the cytoplasmic membrane, where the lipophilic ionophore compounds rapidly dissolve into the membrane. Conversely, Gram-negative bacteria are separated from the environment and antimicrobial agents by a lipopolysaccharide layer, outer membrane, and periplasmic space. Thus, as expected, *E.*

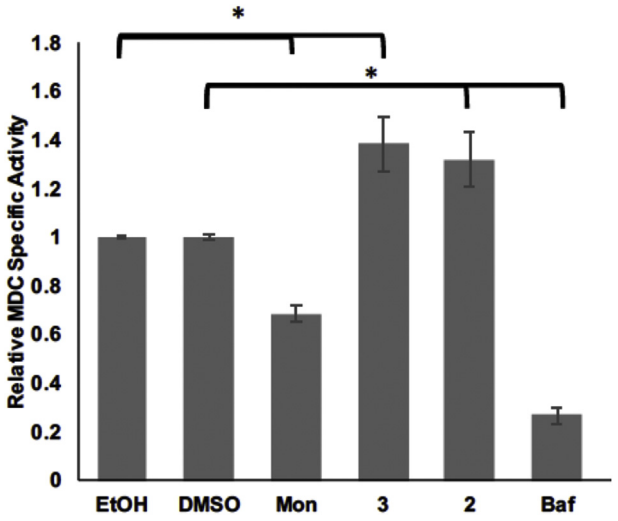

Fig. 5. Compounds **2** and **3** cause accumulation of acidic vacuoles. After treatment of HeLa cells with Compounds **2**, **3**, Mon and Baf A1, MDC fluorescence intensities were measured. MDC values were normalized with PI values and the relative MDC specific activity was determined for each sample compared to the negative controls (EtOH and DMSO). Flourometric analysis of MDC was performed in triplicates and quantitative data was presented as mean ± standard error of mean (s.e.m). *p value < 0.005.

coli, the Gram-negative bacteria of significant importance to food safety and human health, was less susceptible to the isolates **1**–**3**.

From a chemistry point of view, as arenaric acid (**1**) was not as effective as compounds **2** and **3**, one might suggest that the presence of C (25)–C (29) pyran ring and the dideoxy-sugar residue extending from C-27(O) is important for antimicrobial activity. It needs to be emphasized that all the isolated compounds are being reported for the first time from *S. cacaoi*.

Besides being selective antimicrobial agents, polyether ionophores became point of interest for their potential use in cancer chemotherapy over the last decade. One of the breakthrough report suggested that salinomycin, a naturally occurring polyether, inhibits breast cancer growth and metastasis in mice [22]. Moreover, it kills epithelial cancer stem cells, which are resistant to many current chemotherapeutic agents and approaches. Another study reports that salinomycin induces apoptosis in human cancer cells, but not in normal cells such as human T lymphocytes [21]. Mon is another polyether antibiotic, which has also been studied in depth for its anti-cancer effect. Several reports have suggested different molecular mechanisms of salinomycin and Mon probably depending on cell type, such as inhibiting Wnt signaling, elevating oxidative stress, release of caspase activators, inducing apoptosis and modulating autophagy [53–61]. Considering all of these significant studies, characterizing new polyether-type secondary metabolites and their analogs as novel anticancer agents are of great interest. Consistent with this trend, two of our isolates (**2** and **3**) in this study exerted selective toxicity against cancer cells compared to the non-cancerous cells (Table 2).

Apoptosis, controlled necrosis and autophagic cell death are classified cell death pathways. Most of the time cells undergo mixed features of multiple cell death mechanisms suggesting these three cell death pathways do not work in a mutually exclusive manner. Autophagy is primarily known for its bulk degradation of cytoplasmic contents and has a basic role in relieving cellular stress by recycling its content. Cancer cells are more dependent on autophagy than normal cells due to their altered microenvironment, increased metabolic and biosynthetic demand inflicted by their deregulated proliferation [62,63]. Polyether-type compounds like Mon, Nig and lasalocid were reported for their inhibitory actions on lysosomal degradation [11] making them specific autophagy inhibitors at the terminal stage [23].

In this study, the effects of polyethers **2** and **3** were studied on autophagy. The conversion of LC3-I into LC3-II, a central player in autophagosome membrane-bound form, was first evaluated. Levels of LC3-II was compared to actin rather than LC3-I considering the last edition of “Guidelines for the use and interpretation of assays” [38]. Our data suggests that both compounds increase LC3-II levels in all 3

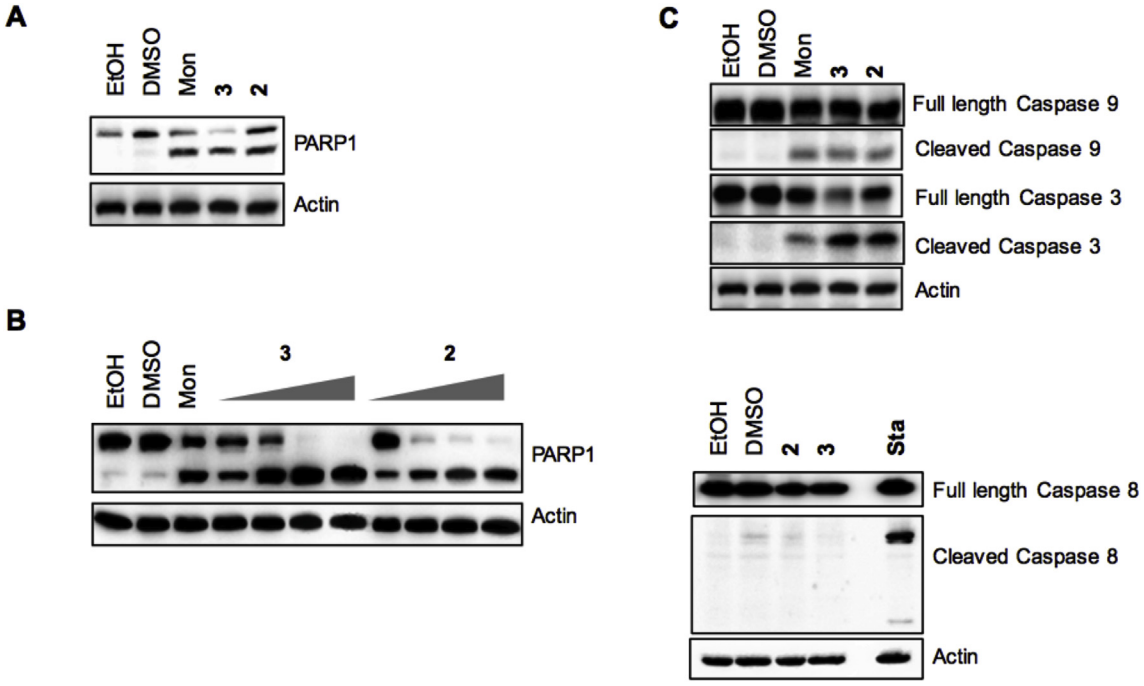

Fig. 6. Compounds **2** and **3** induce apoptosis. The expression level and cleavage of PARP1 in HeLa cells were evaluated in cells treated with **2** and **3** at **(A)** IC_{50} concentration or at **(B)** different doses including ¼, ½, 1X and 2X of IC_{50} doses for 24 h. Actin was used as loading control. **C.** Cleavage products of caspase-9, caspase-3, and caspase-8 were analyzed in cells treated with compounds **2** and **3** at IC_{50} concentration by IB. Staurosporin used at 1 μM concentration for 6 h as positive control. The experiments were repeated three times independently; with one representative result shown.

tested cell lines (Fig. 2A and B). The increased snapshot levels of LC3-II and the accumulation of autophagic vesicles in cells can be associated with an increase in autophagosome synthesis, but can also occur when autophagic flux is blocked, and their degradation rate is reduced in certain cells. Thus in addition to LC3-II levels, the effect of **2** and **3** on p62/SQSTM1 levels were analyzed, as inhibition of autophagy correlates with increased levels of p62/SQSTM1, and similarly decreased p62/SQSTM1 levels are associated with autophagy activation [38]. Here, cells treated with compounds **2** and **3** caused an increase in LC3-II and p62/SQSTM1 (Fig. 2A and B). To further distinguish between increased autophagosome synthesis and inhibited autophagic flux, we examined the effects of **2** and **3** on LC3-II levels in the presence and absence of Baf A1, a proton-ATPase inhibitor that blocks autophagic degradation that does not affect autophagosome formation [64]. It was revealed that LC3-II accumulated as a consequence of impaired autophagic flux and the disrupted degradation of LC3-II, since Baf A1 combination did not change the effect of **2** and **3** on LC3 levels (Fig. 3A). Similarly, there was no significant difference between the average GFP-LC3 puncta numbers per cell in the presence of Baf A1 compared to that in the absence of Baf A1 (Fig. 3B). Interestingly, the data of GFP-LC3 cleavage assay revealed that our compounds increases free GFP levels similar to the autophagy inhibitor Mon, which is contraversial to another autophagy inhibitor Baf A1 (Fig. 3C). Strikingly, both Baf A1, an inhibitor of vacuolar H + ATPase and Mon, which mediates the exchange of protons for potassium or sodium were shown to inhibit macroautophagy trigerring apoptosis [65]. Additionally, it has been clearly shown that cleavage of free GFP from GFP-LC3 can occur depending on the autophagy stimuli, the extent of lysosomal inhibition and the change in lysosomal pH [32]. The induction of autophagy by rapamycin but not starvation was found to increase the free GFP levels, indicating the importance of lysosomal acidity in regulating GFP-LC3 cleavage that produces free GFP [32]. Intriguingly, a well-known autophagy inhibitor chloroquine also increased the free GFP levels at unsaturating doses but not at saturating doses, which suggests that GFP-LC3 degradation occurs in a step-wise manner, in which free GFP fragments are first produced and then degraded their accumulations depend on the lysosomal activity. It would be valuable to dissect the dynamic turnover rates of GFP-LC3 by using saturating doses of our compounds and Mon in this assay; however, solubility of the compounds was the limiting factor to carry out further studies. In summary, we suggest that compounds **2** and **3** inhibit autophagy by disrupting autophagy flux since co-treatment of the compounds with Baf A1 compared to treatments alone did not affect the endogen LC3-II levels (Fig. 3A) and the average of GFP-LC3 puncta numbers per cell (Fig. 3B).

Beclin-1 and Atg proteins are crucial players in the induction and maturation phases of the autophagy pathway. Our results suggest that prolonged treatment of compounds **2** and **3**, unlike Mon, downregulated the levels of these executor proteins of the autophagy pathway in a dose dependent manner (Fig. 4A, B, and C). Furthermore, **2** and **3** significantly enhanced acidic vacuole staining by MDC, which revealed accumulation of acidic autolysosomes instead of neutral autophagosomes caused by Mon or Baf A1 treatment (Fig. 5) [66]. Inhibition of autophagy can be due to several reasons, including inhibition of V-ATPase or ATP2A/SERCA Ca^{2+} pump, depolymerization of microtubules, inhibition of proteins involved during autophagosome and lysosome fusion or altering of lysosomal pH [16,19,66]. Our findings suggest that compounds **2** and **3** have different mechanism of action than Mon, which certainly requires further investigation.

Polyethers have also been reported to induce apoptosis via several mechanisms, such as targeting the intracellular Ca^{2+} homeostasis, induction of reactive oxygen species, releasing cytochrome *c* to the cytosol by outer mitochondrial membrane permeabilization, and cleavage of caspases and PARP-1 [19,20,56]. Caspases-8, -9 and -3 function at the pivotal junctions in apoptosis pathways. While caspase-9 serves in intrinsic pathway, caspase-8 initiates apoptosis in response to extracellular apoptosis-inducing ligands (extrinsic apoptosis). Caspase-3 amplifies the initiation signals of caspase-8 and caspase-9 for apoptosis process [67]. Immunoblot analysis using antibodies that recognize cleaved caspase-3, -8, and -9 fragments indicated that caspase-3 and -9 activity, but not caspase-8 activity, were increased following treatments with compounds **2** and **3** concomitant with cleavage of PARP-1 in a dose dependent way, suggesting induction of intrinsic apoptosis pathway (Fig. 6).

The crosstalk between autophagy and apoptosis needs to be tightly regulated, and one such essential mechanism is known to be the cleavage of caspase-3, to then in turn degrade various autophagy related proteins, like Beclin-1 and Atg3 [68,69]. Other proteases such as calpain-1 have also been reported to utilize Atg proteins as substrates leading to the downregulation of Atg proteins [69,70]. In this study, it was observed that prolonged treatment of **2** and **3** resulted in downregulation of Beclin-1 and some other Atg proteins. This prompted us to hypothesize that the downregulation of Atg proteins by compounds **2** and **3** might be due to the activation of proteases preventing further accumulation of autophagic vesicles, which needs to be further investigated.

From structure-activity relationship perspective, Mon and the isolated compounds (**2** and **3**) have two major differences structurally: i) highly oxygenated (*O*-methyl substituted) polyether framework for compounds **2** and **3**; ii) the presence of 4′-*O*-methyl-α-D-amicetose (sugar) unit in **2** and **3**. These two features might also play crucial roles for the observed activity differences.

Most of the biological activities of polyether ionophores mentioned above are closely related to their ability to form complexes with metal cations (such as calcium) and transport these complexes across lipid bilayers and cell membranes [71]. It has been reported that intracellular Ca^{2+} plays a critical role in the regulation of apoptosis and autophagy [72,73]. Further studies are needed to evaluate the effect of the compounds on the intracellular Ca^{2+} levels and whether apoptosis and autophagic flux blockage induced by them are attributed to Ca^{2+} concentration. As well, after hydrolytic cleavage of the sugar residue, the aglycone needs to be tested to clarify the structural importance of the glycosidic nature, and the number of polyether-type compounds possessing highly diverse chemical frameworks (i.e. different patterns of glycosidation, oxygenation, ring junction etc.) should be evaluated in advance studies. The future studies will be valuable in understanding the global molecular mechanism of cytotoxicity of these polyether antibiotics against cancer cells, their possible connection between autophagy inhibition and activation of apoptosis, and structure-activity relationships.

5. Conclusion

Streptomyces species are rich sources of bioactive compounds. Three compounds with antimicrobial activity were isolated from the marine derived *S. cacaoi*. Due to the structural similarity with known autophagy modulators and anticancer agents, the effects of our compounds were studied against various cancer and non-cancerous cell lines. K41 A (**2**) and the new compound **3**, polyether-type ionophores, exhibited varied cytotoxicity against the entire range of cell lines. Furthermore, both compounds might inhibit autophagy flux in the terminal stage. Interestingly, in contrast to known polyether autophagy inhibitor Mon, these compounds increased acidic compartments in the cells and downregulated the fundamental Atg proteins required for autophagosome formation. Along with this, similar to Mon, compounds **2** and **3** also induced apoptosis in cancer cell lines. Results of the present study suggest that autophagy inhibition and apoptosis induction may play a role in mediating at least some of the antineoplastic effects of these bacterial metabolites.

Declaration of interests

The authors declare that they have no known competing financial

interests or personal relationships that could have appeared to influence the work reported in this paper.

Funding

This research was supported by grants from TUBITAK (109S361) and EBILTEM (2012/BİL/028) (E.B.).

Notes

The authors declare no competing financial interests.

Acknowledgements

We are grateful to Dr. Burcu Erbaykent Tepedelen (Uludag University) for her critical administrative support and Göklem Üner, Recep İlhan, Emre Gezer for their technical assistance. We also thank the Pharmaceutical Sciences Research Centre (FABAL) of Ege University Faculty of Pharmacy for equipmental support.

Appendix A. Supplementary data

Supplementary data to this article can be found online at https://doi.org/10.1016/j.cbi.2019.04.035.

References

[1] D.A. Kevin, D.A.F. Meujo, M.T. Hamann, Polyether ionophores: broad-spectrum and promising biologically active molecules for the control of drug-resistant bacteria and parasites, Expert Opin. Drug Discov. 4 (2009) 109–146.
[2] N. Mizushima, M. Komatsu, Autophagy: renovation of cells and tissues, Cell 147 (2011) 728–741.
[3] S. Alavez, M.C. Vantipalli, D.J. Zucker, I.M. Klang, G.J. Lithgow, Amyloid-binding compounds maintain protein homeostasis during ageing and extend lifespan, Nature 472 (2011) 226–229.
[4] J.Y. Guo, H.Y. Chen, R. Mathew, J. Fan, A.M. Strohecker, G. Karsli-Uzunbas, J.J. Kamphorst, G. Chen, J.M. Lemons, V. Karantza, H.A. Coller, R.S. Dipaola, C. Gelinas, J.D. Rabinowitz, E. White, Activated Ras requires autophagy to maintain oxidative metabolism and tumorigenesis, Genes Dev. 25 (2011) 460–470.
[5] M. Renna, M. Jimenez-Sanchez, S. Sarkar, D.C. Rubinsztein, Chemical inducers of autophagy that enhance the clearance of mutant proteins in neurodegenerative diseases, J. Biol. Chem. 285 (2010) 11061–11067.
[6] E. Wong, A.M. Cuervo, Autophagy gone awry in neurodegenerative diseases, Nat. Neurosci. 13 (2010) 805–811.
[7] V. Romanello, E. Guadagnin, L. Gomes, I. Roder, C. Sandri, Y. Petersen, G. Milan, E. Masiero, P. Del Piccolo, M. Foretz, L. Scorrano, R. Rudolf, M. Sandri, Mitochondrial fission and remodelling contributes to muscle atrophy, EMBO J. 29 (2010) 1774–1785.
[8] L. Gonzalez-Malerva, J. Park, L.H. Zou, Y.H. Hu, Z. Moradpour, J. Pearlberg, J. Sawyer, H. Stevens, E. Harlow, J. LaBaer, High-throughput ectopic expression screen for tamoxifen resistance identifies an atypical kinase that blocks autophagy, Proc. Natl. Acad. Sci. U. S. A 108 (2011) 2058–2063.
[9] V. Deretic, Autophagy in immunity and cell-autonomous defense against intracellular microbes, Immunol. Rev. 240 (2011) 92–104.
[10] B. Levine, N. Mizushima, H.W. Virgin, Autophagy in immunity and inflammation, Nature 469 (2011) 323–335.
[11] B. Grinde, Effect of carboxylic ionophores on lysosomal protein degradation in rat hepatocytes, Exp. Cell Res. 149 (1983) 27–35.
[12] J. Lim, H.-W. Kim, M.B. Youdim, I.J. Rhyu, K.-M. Choe, Y.J. Oh, Binding preference of p62 towards LC3-ll during dopaminergic neurotoxin-induced impairment of autophagic flux, Autophagy 7 (2011) 51–60.
[13] J. Lim, Y. Lee, H.W. Kim, I.J. Rhyu, M.S. Oh, M.B.H. Youdim, Z.Y. Yue, Y.J. Oh, Nigericin-induced impairment of autophagic flux in neuronal cells is inhibited by overexpression of bak, J. Biol. Chem. 287 (2012) 23271–23282.
[14] J. Klose, M.V. Stankov, M. Kleine, W. Ramackers, D. Panayotova-Dimitrova, M.D. Jager, J. Klempnauer, M. Winkler, H. Bektas, G.M. Behrens, F.W. Vondran, Inhibition of autophagic flux by salinomycin results in anti-cancer effect in hepatocellular carcinoma cells, PLoS One 9 (2014) e95970.
[15] X. Chen, L. Chen, S. Jiang, S. Huang, Maduramicin induces apoptosis and necrosis, and blocks autophagic flux in myocardial H9c2 cells, J. Appl. Toxicol. 38 (2018) 366–375.
[16] C. Mauvezin, T.P. Neufeld, Bafilomycin A1 disrupts autophagic flux by inhibiting both V-ATPase-dependent acidification and Ca-P60A/SERCA-dependent autophagosome-lysosome fusion, Autophagy 11 (2015) 1437–1438.
[17] J. Vallecillo-Hernandez, M.D. Barrachina, D. Ortiz-Masia, S. Coll, J.V. Esplugues, S. Calatayud, C. Hernandez, Indomethacin disrupts autophagic flux by inducing lysosomal dysfunction in gastric cancer cells and increases their sensitivity to cytotoxic drugs, Sci. Rep. 8 (2018).
[18] G. Manic, F. Obrist, G. Kroemer, I. Vitale, L. Galluzzi, Chloroquine and hydroxychloroquine for cancer therapy, Mol. Cell Oncol. 1 (2014) e29911.
[19] H.S. Choi, E.-H. Jeong, T.-G. Lee, S.Y. Kim, H.-R. Kim, C.H. Kim, Autophagy inhibition with monensin enhances cell cycle arrest and apoptosis induced by mTOR or epidermal growth factor receptor inhibitors in lung cancer cells, Tuberc. Respir. Dis. 75 (2013) 9–17.
[20] S.H. Kim, K.Y. Kim, S.N. Yu, S.G. Park, H.S. Yu, Y.K. Seo, S.C. Ahn, Monensin induces PC-3 prostate cancer cell apoptosis via ROS production and Ca2+ homeostasis disruption, Anticancer Res. 36 (2016) 5835–5843.
[21] D. Fuchs, A. Heinold, G. Opelz, V. Daniel, C. Naujokat, Salinomycin induces apoptosis and overcomes apoptosis resistance in human cancer cells, Biochem. Biophys. Res. Commun. 390 (2009) 743–749.
[22] P.B. Gupta, T.T. Onder, G. Jiang, K. Tao, C. Kuperwasser, R.A. Weinberg, E.S. Lander, Identification of selective inhibitors of cancer stem cells by high-throughput screening, Cell 138 (2009) 645–659.
[23] M.J. Yoon, Y.J. Kang, I.Y. Kim, E.H. Kim, J.A. Lee, J.H. Lim, T.K. Kwon, K.S. Choi, Monensin, a polyether ionophore antibiotic, overcomes TRAIL resistance in glioma cells via endoplasmic reticulum stress, DR5 upregulation and c-FLIP down-regulation, Carcinogenesis 34 (2013) 1918–1928.
[24] A.-R. Choi, M.-J. Jung, J.-H. Kim, S. Yoon, Co-treatment of salinomycin sensitizes AZD5363-treated cancer cells through increased apoptosis, Anticancer Res. 35 (2015) 4741–4747.
[25] N. Myers, R.A. Mittermeier, C.G. Mittermeier, G.A. da Fonseca, J. Kent, Biodiversity hotspots for conservation priorities, Nature 403 (2000) 853–858.
[26] E.E. Hames-Kocabas, A. Uzel, Alkaline protease production by an actinomycete MA1-1 isolated from marine sediments, Ann. Microbiol. 57 (2007) 71–75.
[27] L.A. Maldonado, W. Fenical, P.R. Jensen, C.A. Kauffman, T.J. Mincer, A.C. Ward, A.T. Bull, M. Goodfellow, Salinispora arenicola gen. nov., sp nov and Salinispora tropica sp nov., obligate marine actinomycetes belonging to the family Micromonosporaceae, Int. J. Syst. Evol. Microbiol. 55 (2005) 1759–1766.
[28] D. Liu, S. Coloe, R. Baird, J. Pederson, Rapid mini-preparation of fungal DNA for PCR, J. Clin. Microbiol. 38 (2000) 471.
[29] K. Ozcan, S.C. Aksoy, O. Kalkan, A. Uzel, E.E. Hames-Kocabas, E. Bedir, Diversity and antibiotic-producing potential of cultivable marine-derived actinomycetes from coastal sediments of Turkey, J. Soils Sediments 13 (2013) 1493–1501.
[30] A.A. Ajaz, J.A. Robinson, D.L. Turner, Biosynthesis of the polyether ionophore antibiotic monensin-a - assignment of the C-13 and proton nmr-spectra of monensin a by two-dimensional spectroscopy - incorporation of O-18 labeled molecular-oxygen, J. Chem. Soc.-Perkin Trans. 1 (1987) 27–36.
[31] J.H. Jorgensen, J.F. Hindler, New consensus guidelines from the Clinical and Laboratory Standards Institute for antimicrobial susceptibility testing of infrequently isolated or fastidious bacteria, Clin. Infect. Dis. 44 (2007) 280–286.
[32] H.-M. Ni, A. Bockus, A.L. Wozniak, K. Jones, S. Weinman, X.-M. Yin, W.-X. Ding, Dissecting the dynamic turnover of GFP-LC3 in the autolysosome, Autophagy 7 (2011) 188–204.
[33] E. Ebata, H. Kasahara, K. Sekine, Y. Inoue, Lysocellin, a new polyether antibiotic. I. Isolation, purification, physico-chemical and biological properties, J. Antibiot. (Tokyo) 28 (1975) 118–121.
[34] N. Tsuji, K. Nagashima, Y. Terui, K. Tori, Structure of K-41B, a new diglycoside polyether antibiotic, J. Antibiot. (Tokyo) 32 (1979) 169–172.
[35] J.P. Dirlam, J. Bordner, W.P. Cullen, M.T. Jefferson, L. Presseau-Linabury, The structure of CP-96,797, a polyether antibiotic related to K-41A and produced by Streptomyces sp, J. Antibiot. (Tokyo) 45 (1992) 1187–1189.
[36] G.T. Carter, G. Schlingmann, G.B. Kenion, L. Milne, M.R. Alluri, J.D. Korshalla, D.R. Williams, F. Pinho, D.B. Borders, Martinomycin, a new polyether antibiotic produced by Streptomyces salvialis, J. Antibiot. 47 (1994) 1549–1553.
[37] I. Tanida, N. Minematsu-Ikeguchi, T. Ueno, E. Kominami, Lysosomal turnover, but not a cellular level, of endogenous LC3 is a marker for autophagy, Autophagy 1 (2005) 84–91.
[38] D. Kliosnky, Guidelines for the use and interpretation of assays for monitoring autophagy (3rd edition) (vol 12, pg 1, 2015), Autophagy 12 (2016) 443-443.
[39] S.R. Yoshii, N. Mizushima, Monitoring and measuring autophagy, Int. J. Mol. Sci. 18 (2017).
[40] Y. Ichimura, E. Kominami, K. Tanaka, M. Komatsu, Selective turnover of p62/A170/SQSTM1 by autophagy, Autophagy 4 (2008) 1063–1066.
[41] E. Laane, K.P. Tamm, E. Buentke, K. Ito, P. Khahariza, J. Oscarsson, M. Corcoran, A.C. Björklund, K. Hultenby, J. Lundin, M. Heyman, S. Söderhäll, J. Mazur, A. Porwit, P.P. Pandolfi, B. Zhivotovsky, T. Panaretakis, D. Grandér, Cell death induced by dexamethasone in lymphoid leukemia is mediated through initiation of autophagy, Cell Death Differ. 16 (2009) 1018.
[42] Z. Wang, J. Zhang, Y. Wang, R. Xing, C. Yi, H. Zhu, X. Chen, J. Guo, W. Guo, W. Li, L. Wu, Y. Lu, S. Liu, Matrine, a novel autophagy inhibitor, blocks trafficking and the proteolytic activation of lysosomal proteases, Carcinogenesis 34 (2013) 128–138.
[43] W. Hou, J. Han, C.S. Lu, L.A. Goldstein, H. Rabinowich, Autophagic degradation of active caspase-8 A crosstalk mechanism between autophagy and apoptosis, Autophagy 6 (2010) 891–900.
[44] J.M. Gump, A. Thorburn, Autophagy and apoptosis: what is the connection? Trends Cell Biol. 21 (2011) 387–392.
[45] Y. Yang, H. Luo, K. Hui, Y. Ci, K. Shi, G. Chen, L. Shi, C. Xu, Selenite-induced autophagy antagonizes apoptosis in colorectal cancer cells in vitro and in vivo, Oncol. Rep. 35 (2016) 1255–1264.
[46] Q. Sun, G.D. Yao, X.Y. Song, X.L. Qi, Y.F. Xi, L.Z. Li, X.X. Huang, S.J. Song, Autophagy antagonizes apoptosis induced by flavan enantiomers from Daphne giraldii in hepatic carcinoma cells in vitro, Eur. J. Med. Chem. 133 (2017) 1–10.
[47] C.J. Dutton, B.J. Banks, C.B. Cooper, Polyether ionophores, Nat. Prod. Rep. 12

(1995) 165–181.
[48] M.N. Novilla, Veterinary toxicology: basic and clinical principles third edition, Ionophores 78 (2018) 1073–1092.
[49] X.C. Cheng, P.R. Jensen, W. Fenical, Arenaric acid, a new pentacyclic polyether produced by a marine bacterium (Actinomycetales), J. Nat. Prod. 62 (1999) 605–607.
[50] G.G. Marconi, B.B. Molloy, R. Nagarajan, J.W. Martin, J.B. Deeter, J.L. Occolowitz, A32390A, a new biologically active metabolite. II. Isolation and structure, J. Antibiot. (Tokyo) 31 (1978) 27–32.
[51] M. Hoshi, T. Endo, Microbial and chemical conversion of antibiotic K41. II. Preparation of K41-DA1,-DA2 and-DA3, deamicetosyl derivatives of antibiotic K41, J. Antibiot. 53 (2000) 1154–1157.
[52] K. Otoguro, A. Ishiyama, H. Ui, M. Kobayashi, C. Manabe, G. Yan, Y. Takahashi, H. Tanaka, H. Yamada, S. Omura, In vitro and in vivo antimalarial activities of the monoglycoside polyether antibiotic, K-41 against drug resistant strains of Plasmodia, J. Antibiot. 55 (2002) 832–834.
[53] W.H. Park, E.S. Kim, C.W. Jung, B.K. Kim, Y.Y. Lee, Monensin-mediated growth inhibition of SNU-C1 colon cancer cells via cell cycle arrest and apoptosis, Int. J. Oncol. 22 (2003) 377–382.
[54] W.H. Park, E.S. Kim, B.K. Kim, Y.Y. Lee, Monensin-mediated growth inhibition in NCI-H929 myeloma cells via cell cycle arrest and apoptosis, Int. J. Oncol. 23 (2003) 197–204.
[55] K. Ketola, P. Vainio, V. Fey, O. Kallioniemi, K. Iljin, Monensin is a potent inducer of oxidative stress and inhibitor of androgen signaling leading to apoptosis in prostate cancer cells, Mol. Canc. Therapeut. 9 (2010) 3175–3185.
[56] K.-Y. Kim, S.-N. Yu, S.-Y. Lee, S.-S. Chun, Y.-L. Choi, Y.-M. Park, C.S. Song, B. Chatterjee, S.-C. Ahn, Salinomycin-induced apoptosis of human prostate cancer cells due to accumulated reactive oxygen species and mitochondrial membrane depolarization, Biochem. Biophys. Res. Commun. 413 (2011) 80–86.
[57] K. Ketola, O. Kallioniemi, K. Iljin, Chemical biology drug sensitivity screen identifies sunitinib as synergistic agent with disulfiram in prostate cancer cells, PLoS One 7 (2012).
[58] D.S. Lu, M.Y. Choi, J. Yu, J.E. Castro, T.J. Kipps, D.A. Carson, Salinomycin inhibits Wnt signaling and selectively induces apoptosis in chronic lymphocytic leukemia cells, Proc. Natl. Acad. Sci. U. S. A 108 (2011) 13253–13257.
[59] T.L. Li, L. Su, N. Zhong, X.X. Hao, D.S. Zhong, S. Singhal, X.G. Liu, Salinomycin induces cell death with autophagy through activation of endoplasmic reticulum stress in human cancer cells, Autophagy 9 (2013) 1057–1068.
[60] L. Tumova, A.R. Pombinho, M. Vojtechova, J. Stancikova, D. Gradl, M. Krausova, E. Sloncova, M. Horazna, V. Kriz, O. Machonova, J. Jindrich, Z. Zdrahal, P. Bartunek, V. Korinek, Monensin inhibits canonical Wnt signaling in human colorectal cancer cells and suppresses tumor growth in multiple intestinal neoplasia mice, Mol. Canc. Therapeut. 13 (2014) 812–822.
[61] H.J. Wu, X.R. Che, Q.L. Zheng, A. Wu, K. Pan, A.W. Shao, Q. Wu, J.M. Zhang, Y. Hong, Caspases: a molecular switch node in the crosstalk between autophagy and apoptosis, Int. J. Biol. Sci. 10 (2014) 1072–1083.
[62] J.D. Rabinowitz, E. White, Autophagy and metabolism, Science 330 (2010) 1344–1348.
[63] E. White, The role for autophagy in cancer, J. Clin. Investig. 125 (2015) 42–46.
[64] D.C. Rubinsztein, A.M. Cuervo, B. Ravikumar, S. Sarkar, V. Korolchuk, S. Kaushik, D.J. Klionsky, In search of an "autophagomometer, Autophagy 5 (2009) 585–589.
[65] P. Boya, R.A. Gonzalez-Polo, N. Casares, J.L. Perfettini, P. Dessen, N. Larochette, D. Metivier, D. Meley, S. Souquere, T. Yoshimori, G. Pierron, P. Codogno, G. Kroemer, Inhibition of macroautophagy triggers apoptosis, Mol. Cell Biol. 25 (2005) 1025–1040.
[66] Z.H. Wang, L. Li, Z.L. Peng, Z.L. Duan, [Effect of autophagy gene Beclin 1 on the growth of cervical cancer HeLa cells in vitro and vivo], Zhonghua Zhongliu Zazhi 33 (2011) 804–809.
[67] P. Hensley, M. Mishra, N. Kyprianou, Targeting caspases in cancer therapeutics, Biol. Chem. 394 (2013) 831–843.
[68] M. Djavaheri-Mergny, M.C. Maiuri, G. Kroemer, Cross talk between apoptosis and autophagy by caspase-mediated cleavage of Beclin 1, Oncogene 29 (2010) 1717–1719.
[69] O. Oral, D. Oz-Arslan, Z. Itah, A. Naghavi, R. Deveci, S. Karacali, D. Gozuacik, Cleavage of Atg3 protein by caspase-8 regulates autophagy during receptor-activated cell death, Apoptosis 17 (2012) 810–820.
[70] S. Luo, D.C. Rubinsztein, Apoptosis blocks Beclin 1-dependent autophagosome synthesis: an effect rescued by Bcl-xL, Cell Death Differ. 17 (2010) 268–277.
[71] J.L.C.M. Dorne, M.L. Fernandez-Cruz, U. Bertelsen, D.W. Renshaw, K. Peltonen, A. Anadon, A. Feil, P. Sanders, P. Wester, J. Fink-Gremmels, Risk assessment of coccidostatics during feed cross-contamination: animal and human health aspects, Toxicol. Appl. Pharmacol. 270 (2013) 196–208.
[72] M.W. Harr, C.W. Distelhorst, Apoptosis and autophagy: decoding calcium signals that mediate life or death, Cold Spring Harb. Perspect. Biol. 2 (2010) a005579.
[73] S.S. Smaili, G.J. Pereira, M.M. Costa, K.K. Rocha, L. Rodrigues, L.G. do Carmo, H. Hirata, Y.T. Hsu, The role of calcium stores in apoptosis and autophagy, Curr. Mol. Med. 13 (2013) 252–265.